Supplementary Files

1. 3D printing of HAc-Alg and HAc-Alg/CaP hydrogels in air

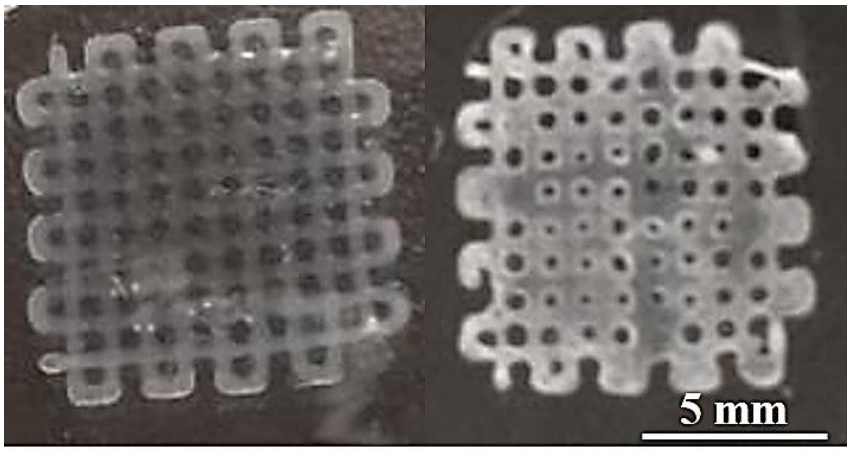

Supplementary Figure 1. HAc-Alg/CaP scaffold directly printed on a glass slide. Left: one layered structure of the scaffold, Right: three-layered structure of the scaffold. During 3d printing, the HAc-Alg ink with (NH4)2HPO4 was deposited on the surface of a glass slide, followed by UV crosslinking. The printed scaffolds were treated in CaCl2 solution for physical crosslinking of alginate and mineralization. The one-layer scaffold could maintain its meshed structure. However, for a scaffold with multi-layered structure, the top layers were collapsed during printing, being merged with the bottom layers.

2. Detailed information of CaP nanoparticles formed in HAc-Alg/CaP hydrogels

Particle size and distribution of HAc-Alg/CaP hydrogels

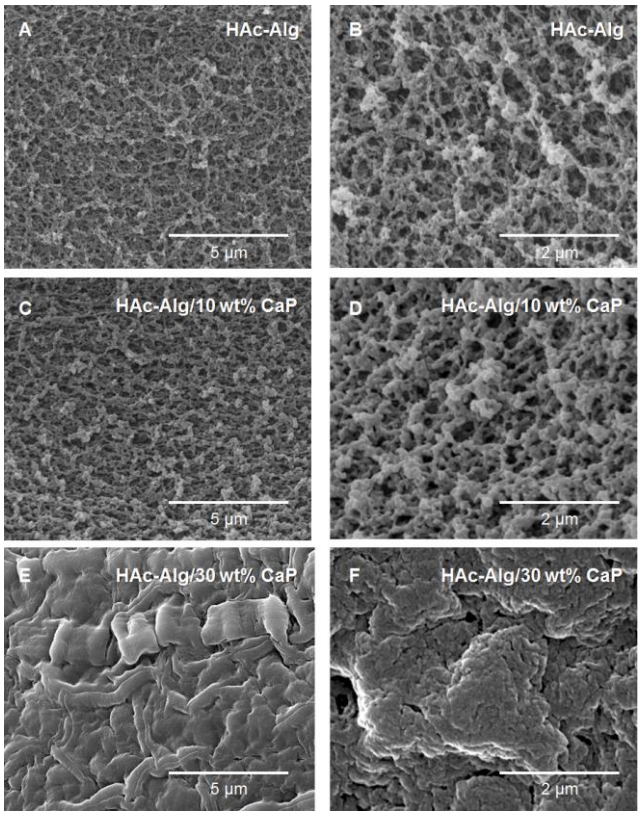

Supplementary Figure 2. High resolution SEM images of (A,B) HAc-Alg hydrogel scaffolds ; (C,D) HAc-Alg/ 10wt% CaP composite hydrogel scaffolds; (E,F) HAc-Alg/ 30wt% CaP composite hydrogel scaffolds. The average particle size of hydrogels was determined by analysing the SEM images. The average particle size of calcium carbonate for HAc-Alg was too small to be measured using the SEM image at x 50,000 magnification. For HAc-Alg/10wt% CaP, the average particle size is ~60 nm. In case of HAc-Alg/30wt% CaP, the average particle size was determined using both SEM and TEM images, resulting particle size is ~60 nm in diameter. Based on the particle size analysis, the increased CaP content is likely attributed to the increased number of CaP particles instead of the crystal growth of nanoparticles.

Supplementary Table 1. Theoretical and actual calcium phosphate (CaP) content of HAc-CaP hydrogels and the average size of CaP nanoparticles
*Ca/P ratios were calculated from both quantitative EDS analysis and XRD phase analysis.

	HAc-Alg/CaP		pHAc-CaP [1]	
	10 wt% CaP	**30 wt% CaP**	**10 wt% CaP**	**30 wt% CaP**
Reactants	$CaCl_2$ 0.153 M 10 ml (gelatin bath)		$CaCl_2$ 0.041 M + H_3PO_4 0.024 M	$CaCl_2$ 0.153 M + H_3PO_4 0.024 M
	$(NH_4)_2HPO_4$ 0.024 M 2-3 ml (ink)	$(NH_4)_2HPO_4$ 0.092 M 2-3 ml (ink)		
pH	7 ~ 8		~ 11	
Temperature	Room temperature			
Reaction time	20 min		3 hr	
Actual mineral content	~ 14 wt%	~ 32 wt%	~ 12 wt%	~ 33 wt%
Average particle size	~ 60 nm	~ 60 nm	~ 50 nm	200 – 350 nm

Supplementary Table 2. Comparison of *in situ* precipitation conditions of HAc-Alg/CaP in this work with those of pHAc-CaP in our previous study [1]

HAc-Alg/CaP hydrogels	**Intended CaP contents (wt%)**	**CaCl (M)**	**$(NH_4)_2HPO_4$ (M)**	**Theoretical Ca/P ratio**	**Actual mineral content (wt%)**	**Actual Ca/P ratio***	**Average Nanoparticle size (nm)**
HAc-Alg	0		0	N.A.	0	N.A.	N.A.
HAc-Alg/ 10wt% CaP	10	0.153	0.024	1	14	0.5 ~ 1	58 ± 10
HAc-Alg/ 30wt% CaP	30		0.092	1	32		60 ± 9

EDS analysis of HAc-Alg/CaP hydrogels

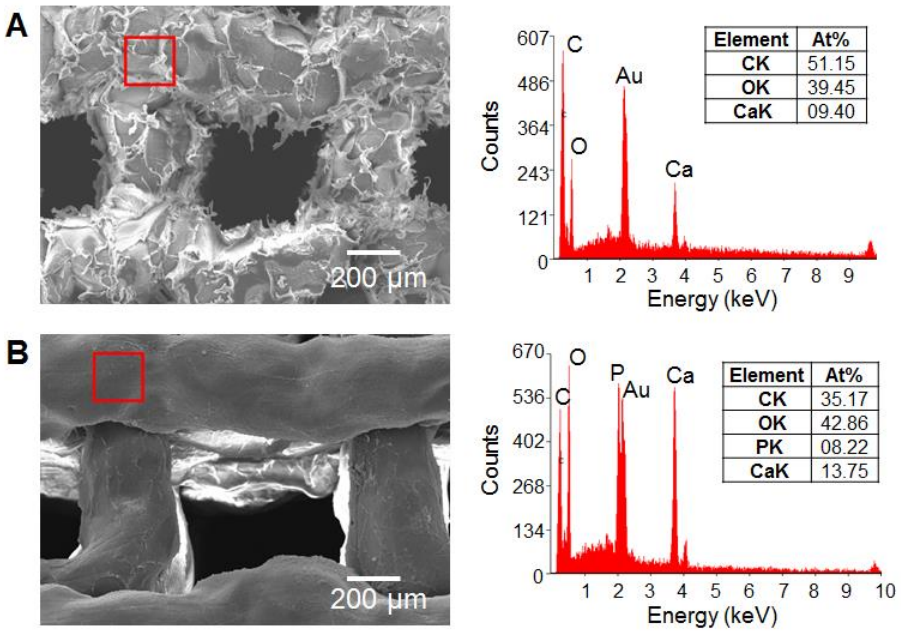

Supplementary Figure 3. SEM images and EDS spectra of (A) HAc-Alg and (B) HAc-Alg/30wt% CaP. HAc-Alg contains a significant amount of calcium due to crosslinking of alginate as well as the existence of calcium carbonate. Because of calcium in alginate, the ratio of Ca/P in HAc-Alg/30wt% CaP is found to be ~1.6. Thus, the Ca/P ratios of CaP nanoprecipitates should be determined using TEM and corresponding EDS analysis instead of SEM.

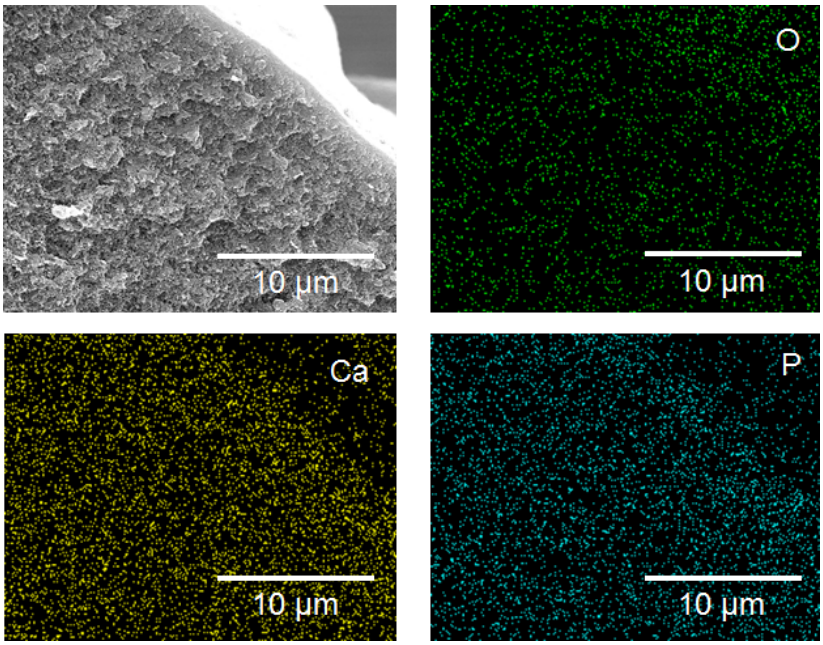

Supplementary Figure 4. Cross-section image of HAc-Alg/30wt% CaP with EDS mapping analysis. Calcium and phosphorous atoms are found throughout the thickness of printed hydrogel filaments, indicating that nanoparticles were successfully formed and uniformly distributed in the whole hydrogel matrix.

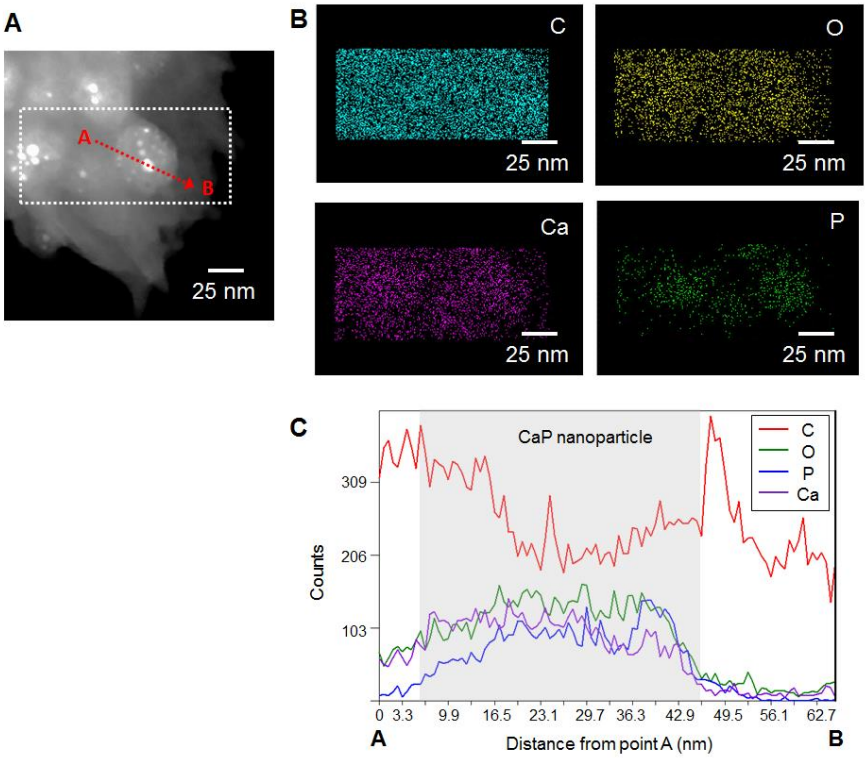

Supplementary Figure 5. (A) TEM image of CaP nanoparticles in the HAc-Alg/30wt% CaP hydrogels, (B) EDS mapping analysis of the nanoparticles from the selected region indicated in the TEM image and (C) EDS line profile analysis of the selected nanoparticle from point A to point B. From the EDS analysis, the Ca/P ratio of CaP nanoparticles was determined as ~0.6.

Determination of mineral contents for composite hydrogels

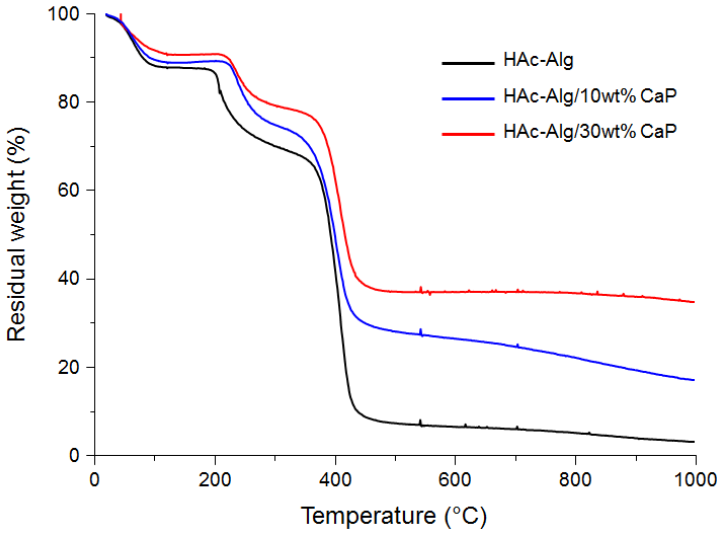

Supplementary Figure 6. TGA results of HAc-Alg hydrogel (black solid line), HAc-Alg/10wt% CaP (blue solid line) and HAc-Alg/ 30wt% CaP (red solid line)**.** The remaining weight at 1000 °C for three types of specimens was used for the calculation of mineral contents for two composite hydrogels. The remaining weight for HAc-Alg should be attributed to calcium oxide and organic ashes after thermal degradation, which was used for the baseline of other two hydrogels.

3. Mechanical behavior and swelling ratio of HAc-Alg and HAc-Alg/CaP hydrogels

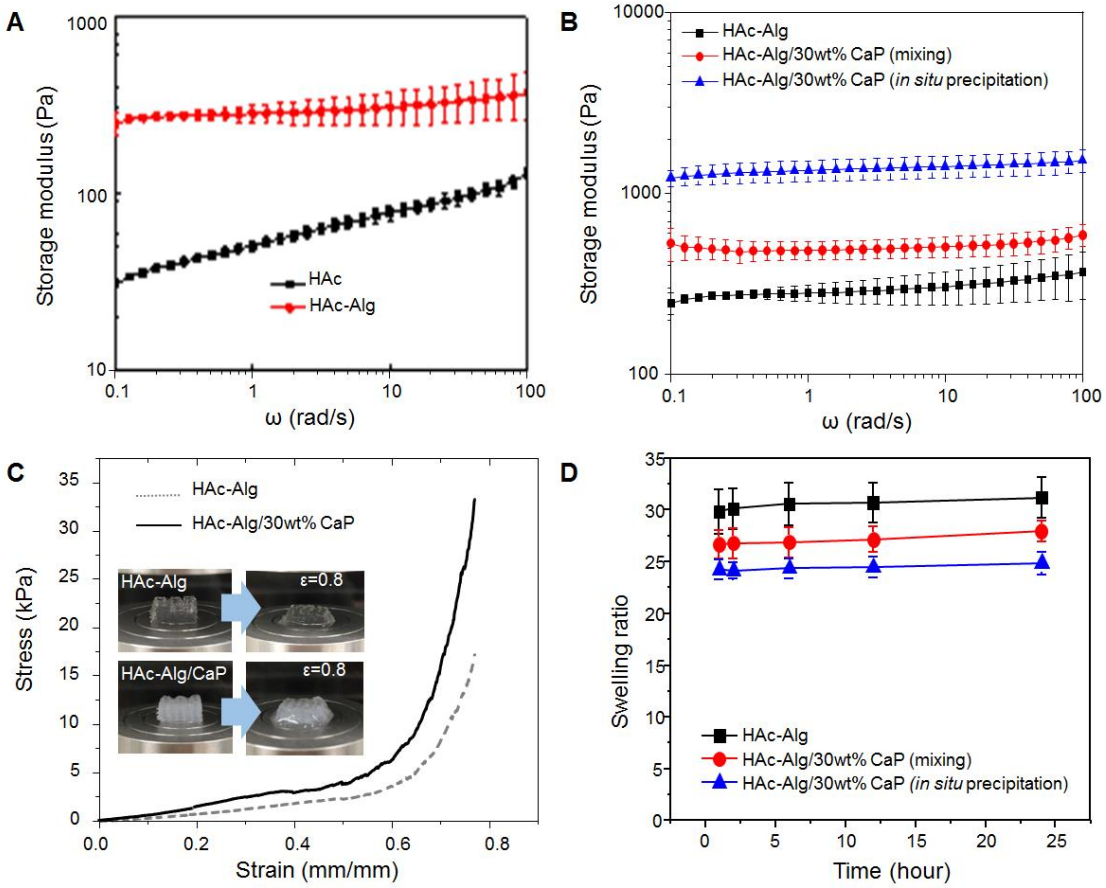

Supplementary Figure 7. (A) Storage modulus over frequency of HAc and HAc-Alg hydrogels, (B) Storage modulus over frequency with different CaP amount, (C) compressive stress-strain curves of 3D printed HAc-Alg and HAc-Alg/30wt% CaP scaffolds. (inset: optical images of hydrogel scaffolds before and after deformation at $\varepsilon = 0.8$), and (D) swelling ratios of three hydrogel specimens: HAc-Alg, HAc-Alg/30wt% CaP by physical mixing of CaP nanoparticles and HAc-Alg and HAc-Alg/30wt% CaP by *in-situ* precipitation ($n > 3$). There are significant differences between any pair-wise comparisons, implying that HAc-Alg/30wt% CaP by *in-situ* precipitation shows remarkable improvement on mechanical and swelling behavior.

4. Detailed information on *in vitro* stability of HAc-Alg and HAc-Alg/CaP scaffolds

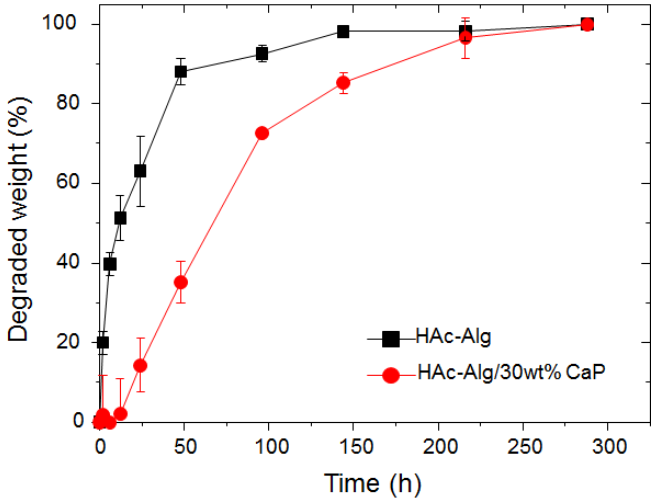

Supplementary Figure 8. Weight loss over incubation time after hydrogel scaffolds were immersed in hyaluronidase solution. The weight loss of hydrogels was calculated from **Figure 6A** of the main manuscript, with the assumption that only enzymatic degradation of hyaluronic acid causes weight reduction.

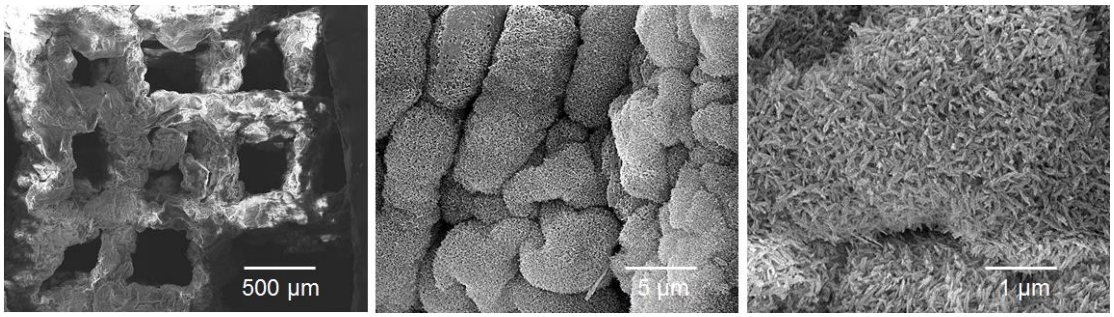

Supplementary Figure 9. SEM images of HAc-Alg/30 wt% CaP composite hydrogel scaffolds after 2 weeks of degradation. The degraded specimens were fully dehydrated using critical point dryer and coated with gold. The surface of HAc-Alg/30 wt% CaP clearly exhibits needle-like nanocrystals, which is well-known to be the morphology of apatite.

5. Detailed information on biological behavior of HAc-Alg/CaP hydrogels

Cell attachment and morphologies of fibroblasts, L929

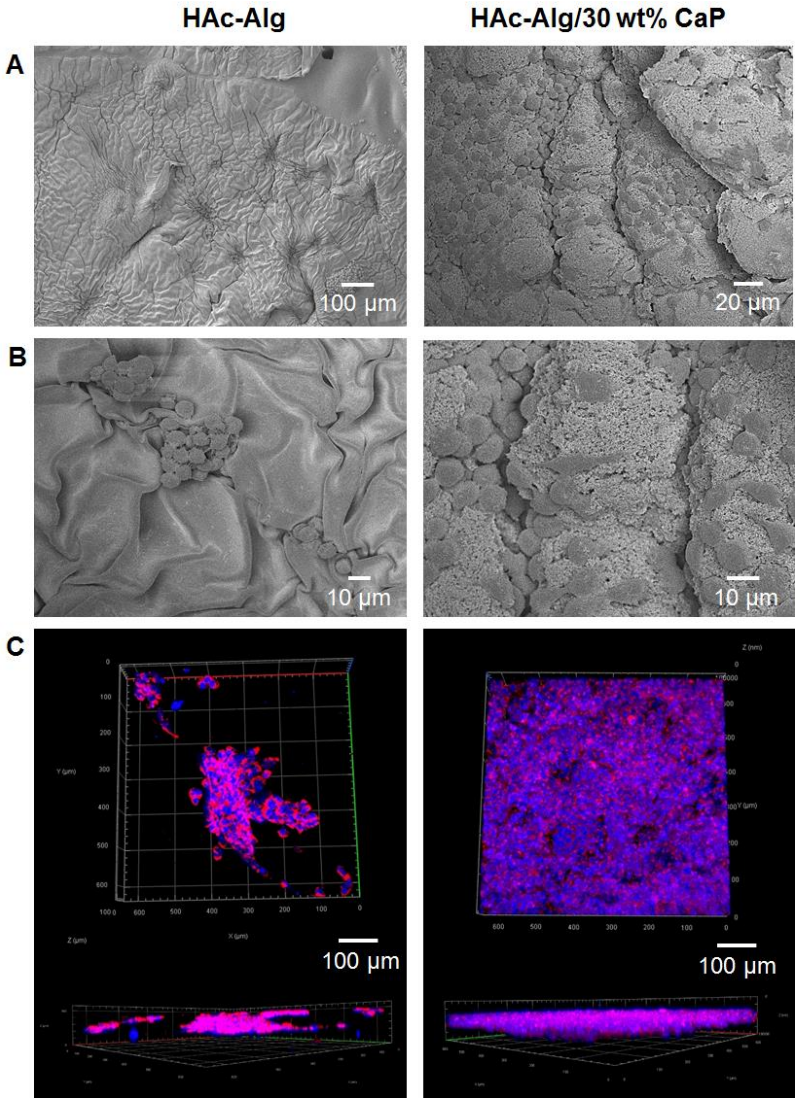

Supplementary Figure 10. (A-B) SEM images of L929 cells on the surfaces of HAc-Alg and HAc-Alg/30wt% CaP after 3 days of culturing and (C) CLSM images of L929 fibroblasts cultured on HAc-Alg and HAc-Alg/30wt% CaP after 3 days of culturing. Cells didn't fully cover the surface of HAc-Alg/30wt% CaP after 3 days of culturing, showing significant local variation of cell density. On the other hand, cells on HAc-Alg didn't attach to the surface well, forming cell clusters. Cell morphologies of two hydrogel surfaces are also different: globular cells on HAc-Alg vs. elongated and flattened cells on HAc-Alg/30wt% CaP.

6. Detailed information on biological behavior of HAc-Alg/CaP hydrogels

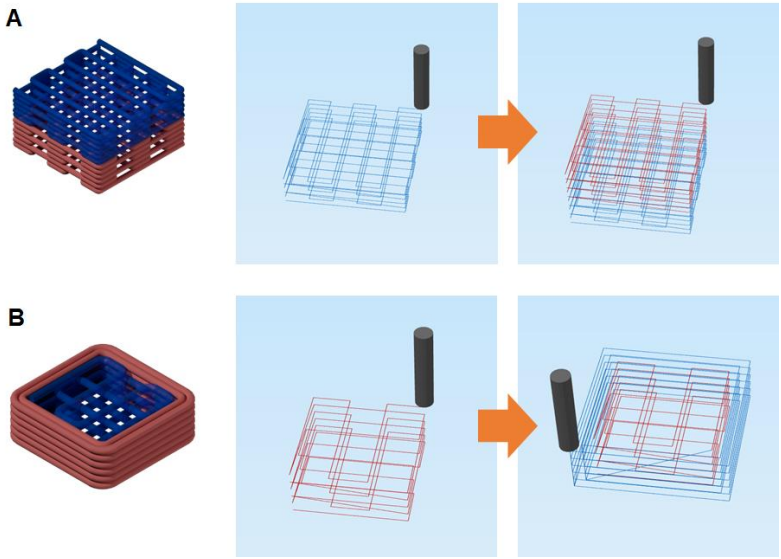

Supplementary Figure 11. Schematics of two bi-material porous scaffolds with corresponding printing sequences: (A) Bi-layered porous scaffold and (B) core-shell porous scaffold.

7. Degree of methacrylation for GM-HAc used in this study

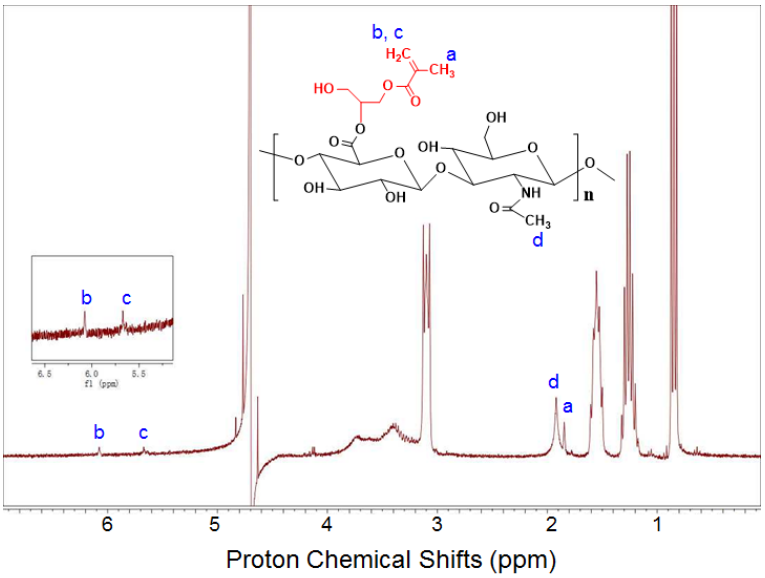

Supplementary Figure 12. H^1NMR spectra of GM-HAc, assigning methacrylate protons and methyl protons to chemical shifts. GMHA were dissolved in deuterium oxide (Sigma-Aldrich, Singapore) at a concentration of 5 mg/mL prior to the test. The H^1NMR spectra was recorded by Bruker Avance Ⅱ 300MHz (Bruker, Germany). The methacrylation of HAc can be determined by the existence of three proton chemical shifts (δ = ~1.85, ~5.65, and ~6.1). The approximate percent of methacrylation (a ratio of methacrylate protons (a) to methyl protons (d)) was calculated from the relative integrations of the methacrylate protons and methyl protons of HAc (two peaks at ~ 1.9 ppm) [2-3]. The linear fitting function of MestReNova software was used for deconvolution and integration of those two peaks. Based on the calculation, the degree of methacrylation for GM-HAc in this study was found to be ~15 %.

Supplementary Videos

Supplementary Movie 1: 3D freeform printing of HAc-Alg hydrogels (.avi)

Supplementary Movie 2: 3D freeform printing of HAc-Alg/30wt% CaP hydrogels (.avi)

Supplementary Movie 3: Taking out a HAc-Alg scaffold from the liquidized gelatin bath (.avi)

Supplementary Movie 4: Taking out a HAc-Alg/30wt% CaP scaffold from the liquidized gelatin bath (.avi)

References

1. Jeong, S. H.; Koh, Y. H.; Kim, S. W.; Park, J. U.; Kim, H. E.; Song, J., Strong and Biostable Hyaluronic Acid-Calcium Phosphate Nanocomposite Hydrogel via in Situ Precipitation Process. *Biomacromolecules* **2016,** *17* (3), 841-51.
2. Leach, J. B.; Bivens, K. A.; Patrick, C. W.; Schmidt, C. E., Photocrosslinked hyaluronic acid hydrogels: Natural, biodegradable tissue engineering scaffolds. *Biotechnol Bioeng* **2003,** *82* (5), 578-589.
3. Bencherif, S. A.; Srinivasan, A.; Horkay, F.; Hollinger, J. O.; Matyjaszewski, K.; Washburn, N. R., Influence of the degree of methacrylation on hyaluronic acid hydrogels properties. *Biomaterials* **2008,** *29* (12), 1739-1749.